The pH Threshold in the Dissolution of β-Lactoglobulin Gels and Aggregates in Alkali

Ruben Mercadé-Prieto, William R. Paterson, and D. Ian Wilson*

Department of Chemical Engineering, New Museums Site, Pembroke Street, Cambridge, CB2 3RA, United Kingdom

Received November 20, 2006; Revised Manuscript Received January 29, 2007

The existence of a practical minimum pH for the dissolution of heat-induced whey gels in alkaline solutions has been studied using β-lactoglobulin (βLg) as a model protein. A sharp transition in solubility was observed between pH 11 and 12; this transition shifts to higher pHs for gels formed at higher temperatures and for longer gelling times. The breakdown reactions of heat-induced aggregates in alkali were monitored with size exclusion chromatography. The destruction of large aggregates was faster at higher pH and also showed a transition between pH 11 and 12. Using tryptophan fluorescence and near- and far-UV circular dichroism, this transition was assigned to the base-induced denaturation observed in solutions of aggregates (p*K* 11.53). It is suggested that the high protein repulsion caused by the large number of charges at pH > 11.5 drives the unfolding of the protein and the disruption of the intermolecular noncovalent bonds. Concentrated urea and GuHCl were found to be less effective than a pH 12 solution in destroying large aggregates. Aggregates formed for a long time (80 °C for 24 h) contained a larger number of intermolecular disulfide bonds that hinder the dissolution process. Gels formed at low temperatures (65 °C for 60 min), with fewer intermolecular noncovalent bonds, showed a similar solubility−pH profile to that observed for the base-induced denaturation of unheated β-lactoglobulin (βLg) (p*K* 10.63).

Introduction

The aggregation and gelation of whey proteins has been the focus of extensive research in the past decade.[1] On the other hand, the cleavage of these biomacromolecues has received little attention, with the exception of work such as that by Mackie et al.[2] on the displacement of proteins by surfactants at interfaces. While intermolecular β-sheets can be formed at interfaces,[3] the extent of protein aggregation is low compared to that of a typical heat-induced gel. Our initial motivation for studying the breakup of these supramolecular structures is to have a better understanding of the alkaline cleaning of the proteinaceous fouling layers formed during the heat treatment of milk. Since the early work by Jennings,[4] the cleaning process has been extensively characterized phenomenologically,[5−7] but a detailed explanation of the mechanisms involved has been mostly based on hypotheses. We believe that understanding the complex processes underlying the dissolution of a protein gel is of value to the general subject of protein superstructures and surpasses the aim of a cleaning study.

It is necessary to introduce the dissolution of rubbery polymers in good solvents, as these represent the closest related systems where there exists a significant degree of understanding.[8−10] The dissolution of a rubbery polymer differs from the typical dissolution of a chemical (e.g., dissolution of a NaOH pellet in water) because the rate at which soluble polymeric material arrives at the interface is slow compared to the rate of mass transfer through the boundary layer. The reason is because some polymers are so large that the time needed to free themselves from the polymer matrix and to reach the boundary layer is not negligible.[10] Terms like reptation and disentanglement are used to explain the slow motion of the polymer chains inside the matrix. However, there are significant differences from the dissolution of a whey protein gel in alkali. Most of the polymers studied to date have been dissolved in good solvents and no reaction has been involved; an exception is the alkaline dissolution of Novolacs, but their chain size is usually too small to produce entanglements.[11] In addition, the polymers used are usually highly monodispersed, unlike protein aggregates, and they lack the complex secondary and tertiary structure of proteins. Moreover, in rubbery polymers the chains are mostly hindered by physical interactions (i.e., entanglements), while in a protein system chemical interactions also play a role. One of the major differences, however, between the dissolution of a rubbery polymer and of a protein gel is the fact that the size of the chain remains unchanged during dissolution of polymers while the size of the clusters is greatly reduced in protein gels. Breakdown reactions are essential for the dissolution of a percolating protein gel.

In this paper, we study these breakdown reactions and the role they play given that they can be considered essential for the dissolution of whey protein gels. This idea is linked with the observation that there appears to exist a pH below which the dissolution rate is very small and above which the dissolution rate increases quickly.[5] The dissolution rate is never zero, as there is always a fraction of very weakly bounded or unbounded protein in the gel that eventually is dissolved. This kind of dissolution pH threshold was observed in a recent swelling study of β-lactoglobulin (βLg) in alkaline conditions.[12] Figure 1 (inset) shows the simulated equilibrium swelling degree (*Q*) at different pH and NaCl concentrations. The dotted line is the approximate locus above which dissolution became noticeable before swelling equilibrium was reached. Since the dotted line is a function of two variables, pH and *Q*, we infer a "double dissolution threshold" observed at pH 11−12 and at $Q \sim 17$ (between 0.285 and 0.415 M NaCl). The nature of this second *Q* threshold will not be discussed here, as it is the subject of current work.

* To whom correspondence should be addressed. Tel.: +44 1223 334791; fax: +44 1223 334796; e-mail: diw11@cam.ac.uk.

10.1021/bm061100l CCC: $37.00 © 2007 American Chemical Society
Published on Web 03/23/2007

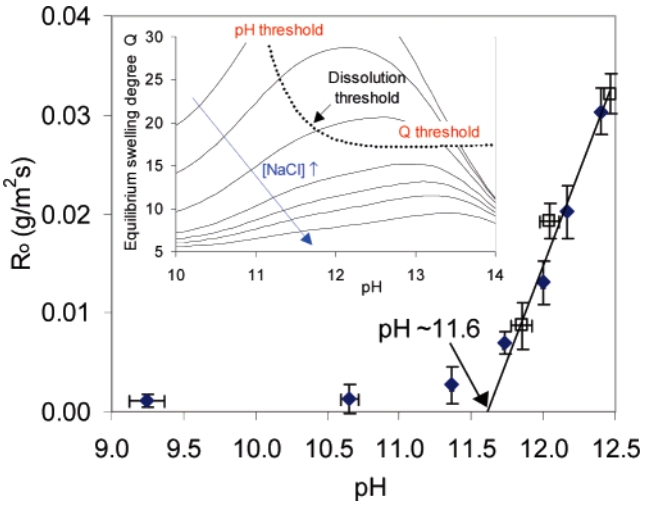

Figure 1. Dissolution rate of βLg gels formed at 80 °C for 20 min (labeled G80/20m) in NaOH (open symbols) or 30 mM Na_2HPO_3 buffered solutions (solid symbols) at 24 °C. The continuous line is the construction used to estimate the dissolution pH threshold. Inset: simulated equilibrium swelling degree Q of βLg gels in solutions at different pH and NaCl concentrations and the observed dissolution threshold, from Mercadé-Prieto et al.[12]

The aim of this paper is to confirm the existence of, and to characterize, the pH threshold for the dissolution of heat-induced βLg gels. βLg is used because of our interest in dairy cleaning, as it is the main protein found in milk-fouling deposits because of its gelling ability and because it is perhaps the protein whose aggregation and gelation behavior is best understood.

Materials and Methods

Materials. β-Lactoglobulin (βLg) was kindly donated by Davisco Foods International, Inc. (Lesueur, MN). The composition of the βLg powder as given by the manufacturer (Lot. JE 003-3-922) was 5.8% moisture, solids (d.b.) 97.4% protein of which 95.0% was βLg; 0.1% fats; and 2.4% ash. Deionized water was used for forming the gels and for the alkali solutions. βLg powder and solutions were stored at 4 °C in airtight containers. Reagents used were of analytical grade (Sigma, Fisher) and were used as received.

Methods. *Gel Formation.* Heat-induced gels (pH 7.45 ± 0.05) were formed inside cylindrical glass capsules, 10.8-mm i.d. and 40-mm high, using well-homogenized 8×10^{-3} M (~15 wt %) βLg solutions, in a water bath at the desired temperature (65−90 °C) for 5−60 min. βLg aggregates were formed using the same procedure but with 2.95×10^{-3} M (~5.5 wt %) βLg solutions, at 80 °C, for 20 min or 24 h. Gels and heated solutions were stored overnight at 4 °C before being used.

Gel Solubility. Gels were solubilized in alkaline solutions using the methods reported previously.[13,14] About 0.04−0.1 g of gel was introduced into a 25-mL centrifuge tube with 20 mL of 75 mM Na_2HPO_3 solution at the desired alkaline pH. In some experiments at pH > 12, NaCl was also added. The protein solution was homogenized at room temperature using an Ultra-Turrax T18 homogenizer for 60 s at 24 000 rpm, followed by 30 min centrifuging at 19 500 rpm below 10 °C. Protein concentration in the supernatant was measured via its absorbance at 280 nm (UV1, Thermo Spectronic). A blank solution without any gel and a blank solution with 0.25 g L^{-1} βLg were used as controls.

Gel Dissolution. Dissolution tests were performed in batch mode at 24 ± 0.1 °C. The dissolution rate was calculated by continuously measuring the increase in protein concentration in the alkali solution (250 mL), using a UV spectrophotometer, while the capsule with the gel was submerged. A detailed description is given in Mercadé-Prieto et al.[14] The gels used were formed at 80 °C for 20 min. Two types of alkali solutions were used: unbuffered NaOH and solutions containing 30 mM Na_2HPO_3 where the pH was adjusted with 4 M NaOH. The dissolution rate at low alkaline pH has been reported to be constant with time;[14] this uniform rate is labeled R_o and was calculated as the average of the rates measured between 10^3 and 10^4 s. The error bars in Figure 1 indicate the standard deviation in these averages. It is not recommended to use NaOH solutions at pH < 12 as the pH can be significantly reduced over the course of the experiment because of the buffering effect of the dissolved βLg. For this reason, phosphate buffers have been preferred for most experiments at low alkaline pHs.

Size Exclusion Chromatography (SEC). The size distribution of the aggregates in the heated βLg solutions and during the breakdown at alkaline pH was measured with SEC in an Äkta FPLC (Amershan Pharmacia) using a prepacked Superdex 200 10/300 GL column, with an exclusion limit of 6×10^5 Da (for globular proteins). A 0.5-mL aliquot of heated βLg solution was diluted 20-fold in a NaOH solution or in a phosphate buffer with a final phosphate concentration of 75 mM at the desired pH. After filtration (0.22 μm PVDF, Millipore), 0.3 mL was injected into the chromatographic system. The column was eluted with a 0.05 M NaCl and 10 mM Na_2HPO_3 (pH 8.9−9.1) solution prepared in Milli-Q water, 0.22 μm PVDF filtered, at a flow rate of 0.65 mL/min. The protein concentration was measured at 280 nm. The heated βLg solutions were incubated at alkaline pH and room temperature (20 ± 2 °C); to follow the breakdown process, chromatograms were taken at different points up to 2 days after mixing. The effect of denaturants on the βLg aggregates was analyzed by mixing 1 mL of the heated βLg solution with 0.36 and 0.56 g urea (final concentration ~4.7 and 6.6 M) and with 0.5 and 0.75 g guanidine hydrochloride (GuHCl) (final concentration ~3.8 and 5.1 M). Samples were incubated overnight at room temperature and were filtered before being analyzed.

Tryptophan Fluorescence. Heated or unheated 2.95×10^{-3} M βLg solutions were diluted 1000× in 75 mM Na_2HPO_3 solution at the desired pH. Solutions were incubated at room temperature for 24 h before being analyzed. The fluorescence emission was recorded between 310 and 400 nm using a Perkin-Elmer LS50B spectrometer upon excitation at 295 nm using a scan speed of 150 nm/min. The excitation and emission slits were 4 and 15 nm, respectively. Three scans were performed and averaged.

Circular Dichroism (CD). CD spectra were recorded at 25 °C using an Aviv model 215 (Aviv Biomedical Inc.). The far UV (190−250 nm) measurements were carried out in a 1-mm cuvette with a protein concentration of 0.27 g/L, while for the near-UV (260−320 nm) measurements a 10-mm path length cuvette was employed with 1.35 g/L solutions. Data shown are the average of five scans. The secondary structure contents were calculated from the far-UV spectra (195/200−250 nm) using the software package CDPro that includes the SELCON3, CDSSTR, and CONTIN programs.[15] The structural content reported is the average of those calculated by the three programs. Between pH 7.5 and 10.93, the reference protein set used was the SP43 set, while a reference set that also includes denatured proteins (SDP48) was used for pHs in the range 10.13−11.99.

For simplicity, the different transitions observed were fitted to a four-parameter sigmoidal curve using the SigmaPlot 9 package to obtain a pK value that can be readily compared between different experiments. The base denaturation of βLg is irreversible, as is the process of dissolution, and it is therefore not an equilibrium as the use of the pK term may normally suggest.

Results

The existence of a practical pH threshold for dissolution is evident in Figure 1 for both NaOH and phosphate-buffered solutions. The dissolution rate, R_o, of βLg gels formed at 80 °C for 20 min (labeled G80/20 m) is almost negligible below pH 11.5 but thereafter it increases substantially with pH. This pH threshold has been estimated to occur at pH ~ 11.6, as

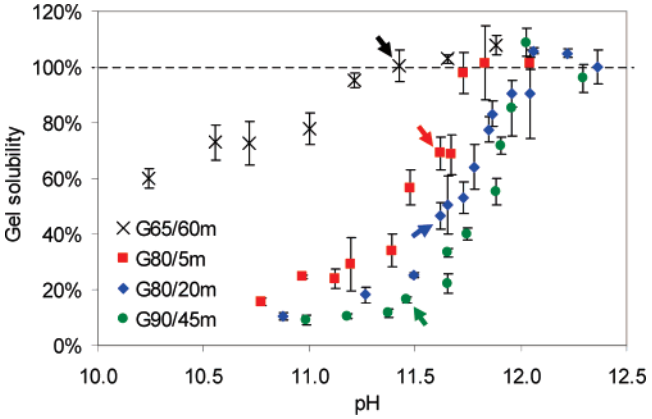

Figure 2. Solubility of gels prepared at different gelling temperatures and times in 75 mM Na_2HPO_3 solutions at different pH. Arrows indicate the pH where similar solubility was found when solubilizing instead with a 6 M urea−0.5 wt % SDS buffer[14] as explained in the text. Notice that these solubilities fall in a similar pH range, 11.4−11.6. Error bars show the standard deviation of four repeats.

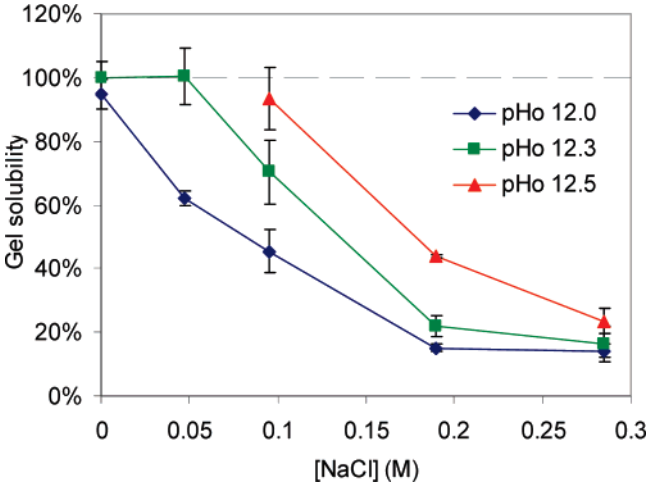

Figure 3. Solubility of G80/20m at high pH in the presence of NaCl. The pH shown is that in the absence of NaCl.

shown in Figure 1. The subsequent experiments were performed to elucidate this behavior.

Gel Solubility. A common technique for obtaining information on the interactions present in a gel is to solubilize the gel using different buffers. Three typical buffers used in the literature are (a) tris-glycine-EDTA pH 8 buffer, used to disrupt H-bonds and electrostatic interactions; (b) 6 M urea and 0.5 wt % sodium dodecyl sulfate (SDS) in buffer a to destroy hydrophobic interactions; and (c) buffer b plus dithiothreitol (DTT), which can in addition reduce disulfide bonds.[13,16] Here, we have performed gel solubility experiments at various alkaline pH using phosphate solutions instead of the above buffers. Gels formed under four different gelation conditions were studied: 65 °C for 60 min (G65/60 m), 80 °C for 5 min (G80/5m), 80 °C for 20 min (G80/20m), and 90 °C for 45 min (G90/45m). We have recently reported the solubility of these gels in buffers (a−c).[14] The solubility of the four gels studied in a was (in order) 22%, 6%, 3%, and 2%, and in b was 100%, 75%, 40%, and 17%, respectively. All were completely soluble in buffer c.

Figure 2 shows the observed solubilities of the four gels at pH 10−12.5. The gel G65/60m behaves differently from the three gels formed at higher temperatures. Its solubility increases continuously above neutral pH, and the p*K* of the transition is estimated at ∼10.3 (not shown). The much higher solubility of G65/60m is expected: at 65 °C, the minimum gelation time is ∼50 min at the protein concentration used here,[14] so this gel is only lightly overcured compared to the other three. The chromatogram of the supernatant at pH 10.23 (solubility ∼60%) showed that almost half of the protein solubilized was in the monomeric or dimeric form, while the nondenaturing SDS-PAGE of the supernatant with tris-glycine-EDTA pH 8 buffer (a) (solubility ∼22%) showed that the soluble part was mainly monomeric (data not shown), suggesting that a significant fraction of the proteins had not yet been incorporated into the gel or were weakly bound. Hence, it is not surprising that this gel is completely soluble in urea-SDS.

The other three gels formed at higher temperatures exhibit a transition, from being relatively insoluble (solubility <20%) to complete solubilization, in a much narrower pH range, between 11 and 12. The transition p*K* of G80/5m, G80/20m, and G90/45m is estimated at 11.5, 11.7, and 11.85 ± 0.1, respectively: the more the gel is overcured, the higher is the p*K*. This transitional p*K* is not only affected by the gelation conditions but is also influenced by the NaCl concentration. The pH threshold (Figure 1, inset) is observed at higher pH for higher NaCl concentrations (the dashed line of the pH threshold is not vertical; it is slightly curved).

Figure 3 shows that for pH's where G80/20m is completely soluble, the solubility decreases markedly with small additions of NaCl back to relatively insoluble values (<20%). The decrease in solubility is not caused by a decrease in the true pH, which at 0.19 M NaCl is less than 0.1 pH units because of the buffering effect of the phosphate. This effect of NaCl and the nature of the *Q* threshold shown in Figure 1 (inset) is the subject of ongoing work.

Another interesting observation is found when comparing the solubilities in buffer b (urea-SDS) and in alkaline phosphate buffers. It is remarkable that the pH of the phosphate buffer that yields the same solubility as buffer b for the four gels studied, shown by arrows in Figure 2, falls in a narrow pH range of 11.4−11.6. However, the four gels present significantly different solubility profiles and, therefore, different amount of intermolecular interactions.

In conclusion, the solubility tests with phosphate buffers exhibit the narrow pH range in which the gels became soluble, in agreement with the pH threshold observed in the dissolution experiments presented in Figure 1.

Breakdown of *β*Lg Aggregates at Alkaline pH. As the gels cannot be readily passed through a chromatographic column, soluble aggregates were used instead. Aggregates were formed at much lower protein concentration than were the gels, but at otherwise similar conditions. The breakdown of the aggregates formed in solution was then monitored using SEC, and the process was simplified by focusing on only two parameters: the fraction of large aggregates (eluted after the excluded volume) and the small oligomers (monomers, dimers, and trimers), without analyzing all the intermediates in between. The main drawback is that each chromatogram takes about 30 min to collect; hence, a good quenching protocol is needed when the breakdown reactions occur very quickly (e.g., at pH > 12). For aggregates formed at 80 °C for 20 min (labeled A80/20m), Figure 4 shows the chromatograms obtained after incubation at different times in an unbuffered NaOH solution at pH 11.66 ± 0.05 and 20 °C. The arrows show the peaks of interest. The relative proportion of the different oligomers, *f*, is estimated as the ratio of the absorbance of the peak of interest

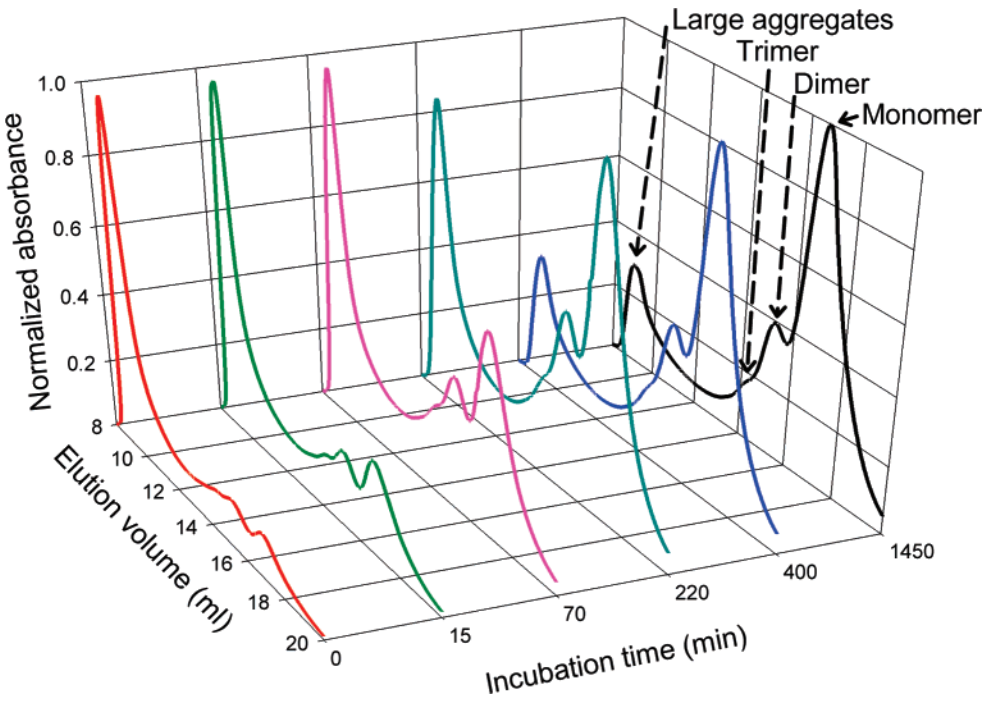

Figure 4. SEC chromatograms for aggregates formed at 80 °C for 20 min (A80/20m) after being incubated in a NaOH solution at pH 11.66 and 20 °C for different times.

to the integral of the absorbance over the eluted volume, as follows:

$$f = \frac{\text{absorbance}_{\text{peak}}}{\int \text{absorbance} \cdot d(\text{elution volume})} \left[\frac{\text{mA}}{\text{mA} \cdot \text{mL}} = \text{mL}^{-1}\right] \quad (1)$$

For A80/20m at neutral pH, the value of *f* obtained for large aggregates was 0.50 ± 0.03 mL^{-1} for five different heated solutions. Figure 5a shows that the *f*-value of large aggregates decreased with time at all alkaline pHs and that there is no significant difference between buffered and unbuffered solutions. Figure 5b shows the corresponding increase in the monomer *f*-value. As expected, the breakdown reactions are faster at higher pHs. The existence of a dissolution pH threshold can again be observed by plotting *f* for the different peaks after an arbitrary time of 300 min (Figure 6). The *f*-value of large aggregates, which can be used as an estimation of the insoluble part of a gel, falls from ~0.38 mL^{-1} at pH < 11 to ~0.02 mL^{-1} at pH > 12, with a transitional p*K* value of 11.55 ± 0.1. While the presence of phosphate does not seem to influence the destruction of the large aggregates, it is evident from Figure 6 that the proportions of monomer, dimer, and trimers formed differ. The ratio of monomer:dimer in NaOH alone (2.04 ± 0.15) is higher than when using the phosphate buffer (1.38 ± 0.15).

As the aggregation process is not finished when heating at 80 °C for 20 min, we also monitored the breakdown reaction of aggregates formed after 24 h at this temperature (labeled A80/24h). Figure 7 shows that, as expected, the initial *f*-value of large aggregates (0.66 mL^{-1}) was larger than for A80/20m (0.5 mL^{-1}), while for the monomers it is even lower (0.04 vs 0.07 mL^{-1}). Likewise, the breakdown of aggregates proceeds much more slowly in A80/24h. For example, at pH 11.90, the *f*-value of large aggregates reaches 0.2 mL^{-1} after 200 min, while for the weaker A80/20m, at pH 11.94, this level is reached after ~15 min. Even at the highest pH studied here of 12.14, more than 50 min is needed for A80/24h. At lower pH, 11.58 and 11.76, a long delay time (~100 min) is observed before the large aggregate fraction starts to decrease (Figure 7). At these pH's, the breakdown reactions proceed even more slowly than for A80/20m (Figure 5).

The ability of denaturants to act as breakdown agents was analyzed by inspecting their impact on the distribution of the different oligomers. Solutions of aggregates with denaturants, urea and GuHCl, were incubated overnight at two different denaturant concentrations. Figure 8 shows the key findings: the large aggregate *f*-value of A80/20m is still about 0.15−0.2 mL^{-1} in 4.7 M urea and 3.8−5.1 M GuHCl, which is similar to the effect of a phosphate buffer at pH ~ 11.6 after 300 min (Figure 6). Only with 6.6 M urea is the monomer *f*-value much larger than that of the large aggregates. The effect of the denaturants on A80/24h is even weaker. Again, the aggregates are destroyed better using 6.6 M urea, but even then the large aggregate *f*-value is still larger than 0.3 mL^{-1}.

Protein Interactions inside the Aggregates. We have demonstrated above the existence of a sharp transition in the dissolution of gels and in the breakdown of aggregates with an average p*K* of ~11.6, and we seek to establish the physical basis for this transition. To determine the nature of the breakdown process, we have to consider first which interactions are present and active in the gel and aggregates. For simplicity, we consider that the gels and aggregates are formed by a mix of noncovalent (i.e., hydrophobic[17,18] and intermolecular β-sheets[19,20]) and covalent (intermolecular disulfide bond[21]) interactions. After prolonged treatment in alkali, all the interactions are likely to be destroyed, yielding a final solution similar to the starting monomeric material. Therefore, we define the time frame of interest from several minutes to a few hours, because the dissolution and solubility experiments (Figures 1 and 2) were performed in less than 3 h. Assuming that by virtue of their weaker nature the breakdown of the noncovalent interactions is much faster than the reduction of the covalent ones, there are three possible scenarios: (1) The noncovalent interactions are destroyed very quickly; the covalent bonds are destroyed during the time frame of interest. (2) The noncovalent interactions are broken down during the time frame of interest,

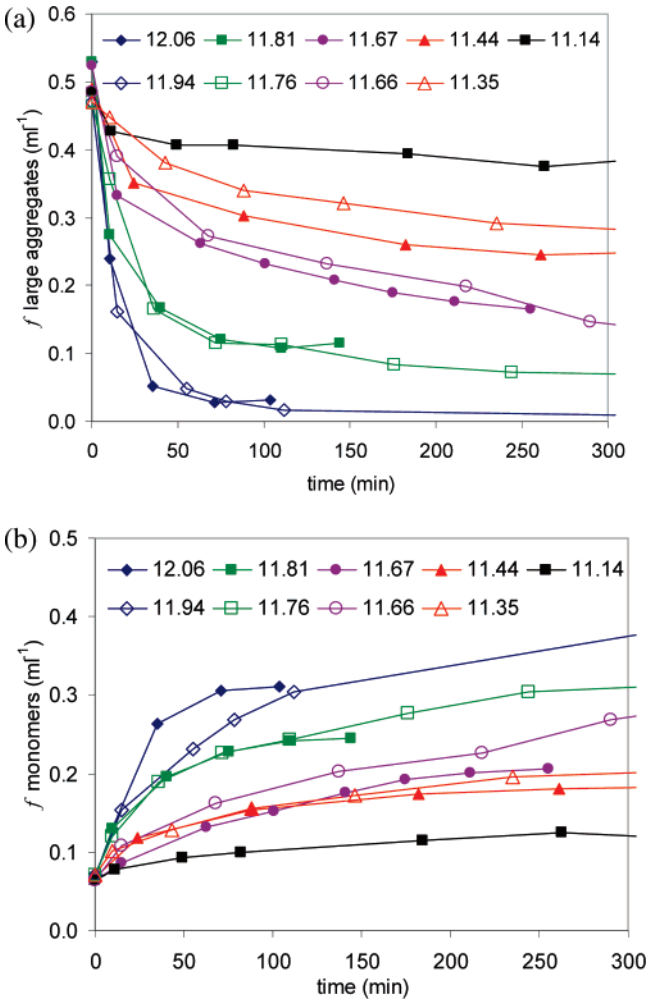

Figure 5. *f*-values of (a) large aggregates and (b) monomers, calculated using eq 1, for A80/20m after incubation in solutions at different pH. Open symbols are for unbuffered NaOH solution; filled symbols are for 75 mM Na_2HPO_3 buffers.

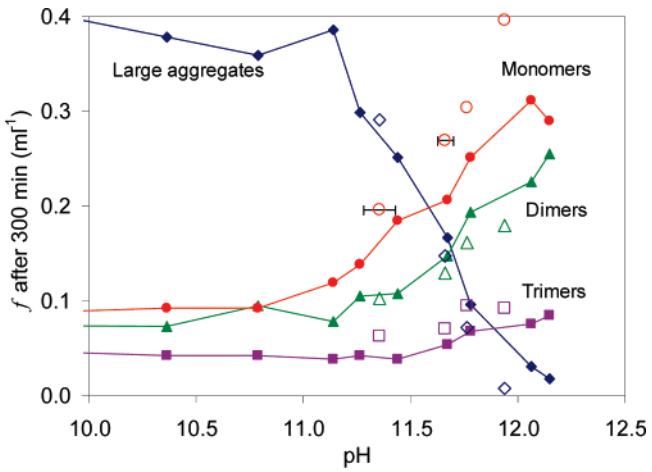

Figure 6. *f*-values of the different SEC peaks for A80/20m incubated in alkaline solutions after 300 min (open symbols for unbuffered NaOH solution; filled symbols, with interpolating lines, for Na_2HPO_3 buffers).

while the covalent bonds are reduced more slowly. (3) Both noncovalent and covalent interactions are destroyed at similar rates.

We have recently studied the breakdown of the covalent interactions via the β-elimination of the disulfide bonds present in βLg.[14] However, the kinetic parameters were obtained for unaggregated βLg and therefore correspond to the β-elimination

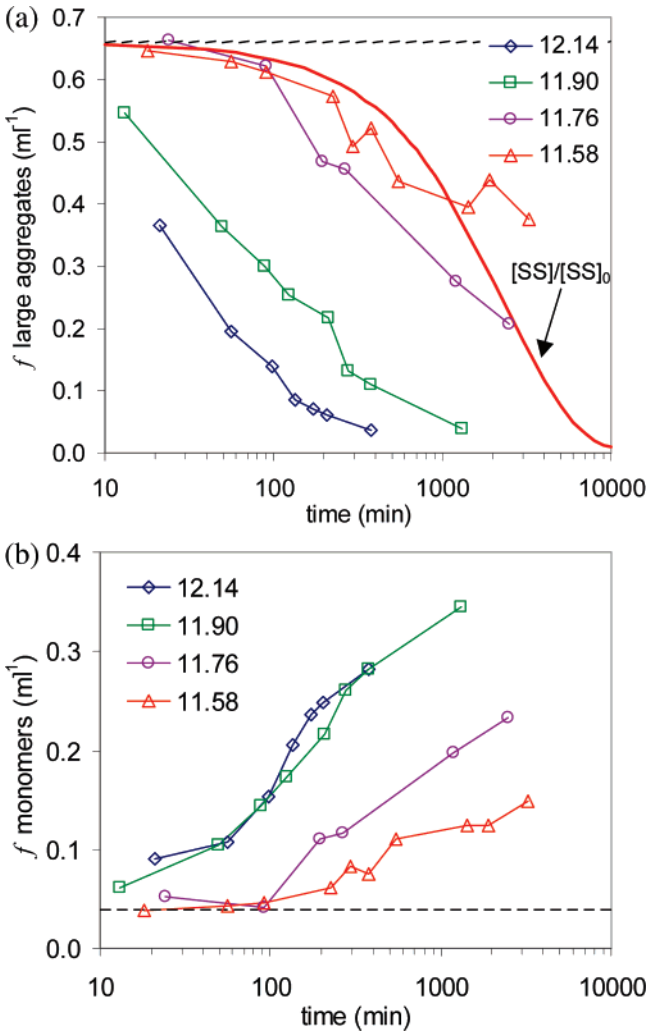

Figure 7. *f*-values of (a) large aggregates and (b) monomers, calculated using eq 1, for A80/24h in solutions at different pH. Dashed lines in a and b represent the initial *f*-value on the untreated A80/24h. The continuous curve in a is $[SS]/[SS]_0$ (corrected to 0.66 as the maximum value) calculated[14] at pH 11.6 and 22 °C. Note the log scale on the time axis.

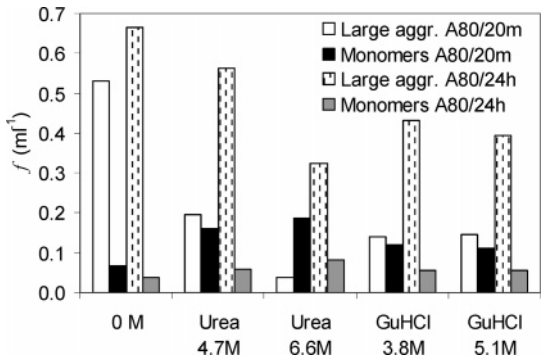

Figure 8. *f*-values of large aggregates and monomers in A80/20m and A80/24h after being incubated overnight in the presence and absence of denaturants at 20 °C.

of the intramolecular disulfide bonds, like all the available data for other proteins.[22] Obtaining the kinetics for the β-elimination of intermolecular disulfide bonds presents a great challenge. Hence, we can only assume that the kinetics for intramolecular disulfide bonds can be applied to the intermolecular ones. In addition, in our kinetic study with βLg, the minimum hydroxide concentration tested was ~0.02 M NaOH (pH 12.3).[14] Therefore, the alkaline conditions of the present study are less severe (pH

< 12.3) than the lowest tested in the earlier β-elimination study. This suggests that the β-elimination reaction is going to be slow, and probably negligible, under the pH and temperature conditions analyzed here. For example, at pH ~ 12 on A80/20m, the *f*-value of large aggregates is reduced to 10% of its value after 40 min (Figure 5a). By comparison, if we calculate the unreacted fraction of disulfide bonds,[14] $[SS]/[SS]_0$, at 22 °C the estimate gives ~95%. A similar value of $[SS]/[SS]_0$ is obtained at pH ~ 11.8 when the *f*-value of large aggregates is reduced to ~24% after 80 min. This suggests that the breakdown of A80/20m follows the type 2 scheme, as the β-elimination reaction is very slow over the time scale where most of the aggregates are destroyed. On the other hand, the breakdown of large aggregates proceeds much more slowly on A80/24h (Figure 7a). This leads to the situation that when 20% of the large aggregates remain at pH 12.14 and 11.90, $[SS]/[SS]_0$ has been reduced to ~80%, significantly more than for A80/20m. At lower pH's (11.76 and 11.58), the two values are indeed quite similar, as shown by the continuous curve in Figure 7a for the calculated $[SS]/[SS]_0$ at pH 11.6. Although the similarity between the $[SS]/[SS]_0$ locus and the *f*-value of large aggregates should not be overemphasized, as both parameters are not directly comparable and because of the assumptions involved in $[SS]/[SS]_0$, it is clear that for A80/24h the β-elimination reactions cannot be neglected. This suggests that the breakdown of A80/24h follows the type 3 scheme, that is, the destruction of the noncovalent and covalent interactions occur in a similar time frame.

It is arguable that the destruction of the noncovalent interactions is going to be related to some degree to the base-induced denaturation of βLg. This conformational change has received less attention than the other conformational changes at acid or neutral pH.[23] Taulier and Chalikian[24] successfully characterized the base-induced denaturation of native βLg using several techniques. They reported transitions occurring between pH 10 and 12 of several properties: structural volume, compressibility, and for both the near- and far-UV CD spectra. These could be explained quite satisfactorily by considering the ionization of the Tyr and Lys residues: the profile of these curves in the alkaline range is similar to the hydrogen ion equilibrium curve for βLg. However, the broad transitions reported between pH 10 and 12 cannot explain the sharp dissolution pH transition observed in this work at pH 11.3−12. It is postulated that this discrepancy could be related to the different nature of aggregates compared to unheated βLg.

Base Denaturation of Aggregates and Unheated βLg. The base-induced denaturation of βLg was characterized in detail using tryptophan fluorescence. Figure 9a shows that the fluorescence intensity of the aggregates A80/20m and A80/24h is higher than for unheated βLg, as has been reported in the literature.[25,26] For unheated βLg, the intensity is observed to decrease along with the base-induced denaturation, while it is known that in the urea-induced denaturation the intensity instead increases.[27] This contrast could be due to the quenching effect of nearby ionized amino acids,[28] like the Tyr_{20} next to Trp_{19}, owing to the increased chain mobility during denaturation. The fluorescence intensity of the aggregates is also reduced at high pH, with a calculated p*K* for the transition of 11.46, compared to 10.68 for the unheated βLg. Inspection of the wavelength at maximum intensity (λ_{max}) confirms that this transition is related to the higher accessibility of the tryptophan residues (Figure 9b); λ_{max} increases from 335 nm for unheated βLg and 342 nm for aggregates at neutral pH to 353 nm at pH > 12, which is typical for completely accessible tryptophans. The p*K* of this

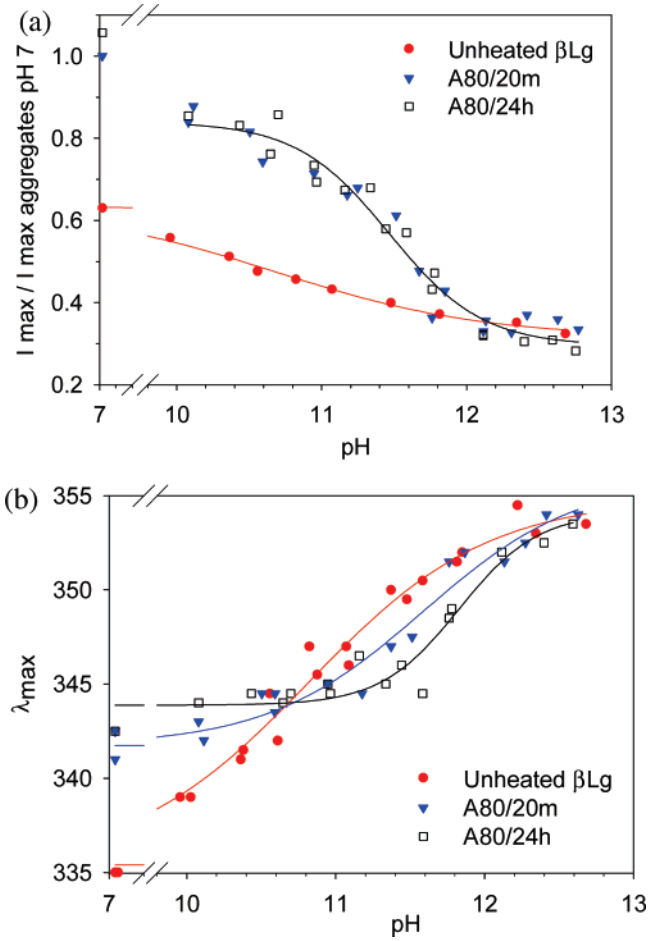

Figure 9. (a) Relative maximum fluorescence intensity of unheated βLg and of aggregates: calculated transition p*K* 10.68 ± 0.06 and 11.46 ± 0.15, respectively. (b) Wavelength at maximum fluorescence intensity. Calculated transition p*K*: 10.82 ± 0.07 for unheated βLg, 11.58 ± 0.12 for A80/20m, and 11.82 ± 0.14 for A80/24h.

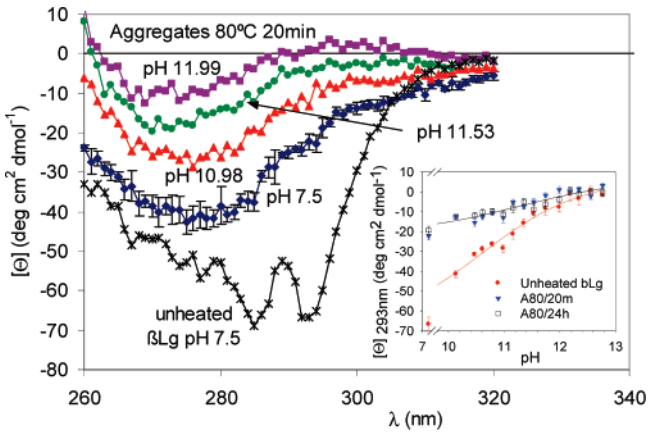

Figure 10. Near-UV CD spectra of unheated βLg at pH 7.5 and of A80/20m in solutions at different pH. Inset: pH dependence of the molar ellipticity at 293 nm. Calculated transition p*K*: 10.6 ± 0.1 for unheated βLg, 11.3 ± 0.4 for both types of aggregates.

transition has been estimated at 10.82 for unheated βLg, 11.58 for A80/20m, and 11.82 for A80/24h.

Circular dichroism (CD) was also used to study the base-induced denaturation, following previous work performed on unheated[24] and on aggregated βLg.[19] Figure 10 shows the near-UV spectra of both unheated βLg and A80/20m. The 293-nm peak of unheated βLg is slightly less pronounced than previously reported,[24,26,27] suggesting that the protein used in the present

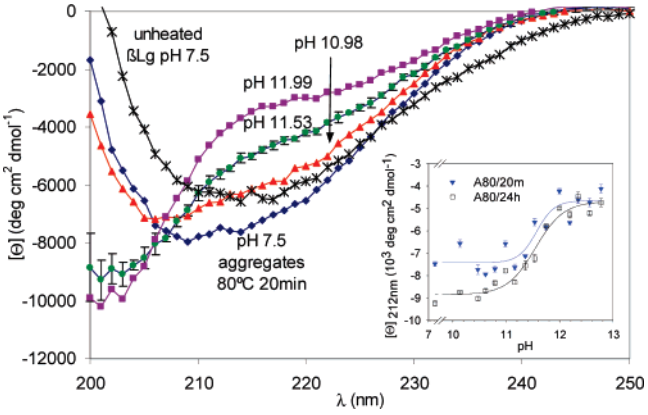

Figure 11. Far-UV CD spectra of unheated βLg at pH 7.5 and of A80/20m in solutions at different pH. Inset: pH dependence of the molar ellipticity at 212 nm. Calculated transition pK: 11.56 ± 0.12 for A80/20m and 11.54 ± 0.07 for A80/24h.

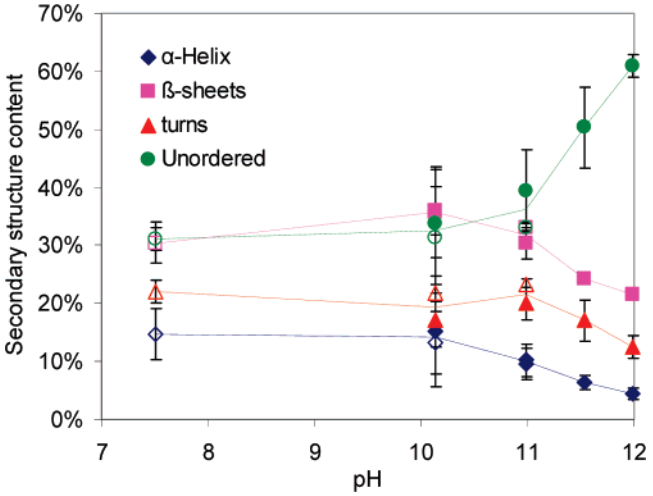

Figure 12. Calculated secondary structure content of A80/20m in solutions at different pH obtained form the CD spectra (Figure 11). Empty points were calculated using the reference set SP43 (43 native proteins), and filled points were calculated using the reference set SDP48 (43 native and 5 denatured proteins).[15]

study is slightly more denatured than the one supplied by Sigma in those studies. The aggregate spectra show the disappearance of the 285- and 293-nm troughs while a new trough at 270−280 nm is formed.[19,26] For the A80/24h, this trough was less intense than for A80/20m shown in Figure 10 (data not shown). By increasing the solution pH, the CD spectra collapsed to the baseline, as observed in the presence of urea,[27] indicating an enhanced mobility of the tryptophan, especially the Trp_{19}, probably because of the disruption of the β-barrel.[19] By following the mean residue ellipticity, $[\theta]$, at 293 nm we can follow the loosening of the tertiary structure with pH. A sigmoidal behavior is again observed, with a pK of 10.6 for unheated βLg and of 11.3 for both types of aggregates. Notice that as the aggregates have lost most of the tertiary structure during the heating process, this transition is not very salient.

The far-UV spectra can provide information about the changes that occur in the secondary structure at high alkaline pH. Figure 11 shows the characteristic trough at 216 nm for structures abundant in β-sheets, namely, the unheated βLg. After the formation of aggregates, the trough shifts to lower wavelengths and to lower $[\theta]$.[26,29] When the aggregates are incubated at high-alkaline pH, the spectra resemble that of an unfolded polypeptide chain,[24] as observed in highly concentrated urea.[27] The base-induced denaturation was followed by monitoring the ellipticity at 212 nm, shown in Figure 11 (inset). The computed pK of the sigmoidal transition is 11.55 for both types of aggregates. The transition of unheated βLg is best monitored at a lower wavelength (e.g., 204 nm) and yields a pK of 10.45 ± 0.07 (data not shown). The calculated secondary structure content for unheated βLg at pH 7.5 is 16.8% α-helix, 32.6% β-sheet, 20.5% β-turn, and 27.0% unordered. These values are consistent with other CD studies,[26,30] although they show significantly less β-sheet content than when using X-ray crystallography, as data at low wavelengths (i.e., 170 nm) are required to successfully characterize β-sheet rich proteins.[31] No statistical difference in the calculated secondary structure was observed between A80/20m and A80/24h.[26] The effect of the pH on the secondary structure of A80/20m is shown in Figure 12. Little change is observed between pH 7.5 and 11, but at higher values all the ordered fractions (α-helix, β-sheet, and β-turn) decrease while the unordered fraction increases to ∼60%. At pH 12, the secondary structure of the unheated βLg and A80/20m are quite similar, although there is 7% less β-sheet and 4% more α-helix for the unheated βLg.

General Discussion. For unheated βLg, the fluorescence and CD data yield a transition pK of 10.63 ± 0.15, confirming previous findings on the base-denaturation transition,[24] as shown by the increased exposure of the tryptophans (Figures 9 and 10) and the loss of secondary structure. The heat treatment of βLg to form aggregates mainly provokes a partial loss of the tertiary structure (higher λ_{max} and lower $[\theta]_{293nm}$) without a significant change of the overall secondary structure, consistent with the formation of a molten globule.[26] However, we cannot distinguish between the β-sheets of the unheated βLg and the intermolecular β-sheets formed during the aggregation process.[20] Our data suggest that the final conformation at the end of the base-induced transition at pH > 12 is essentially the same for unheated βLg and for the aggregates. However, this conformational change is observed at higher pH in aggregates, with an average pK of 11.53 ± 0.15. We suggest that this upward pK shift is related to those interprotein interactions within the aggregates that hinder the unfolding process. Between pH 11 and 12, there is a loss of secondary (especially intermolecular β-sheets) and tertiary structure, causing the disruption of noncovalent interactions that leads to the dissolution threshold observed in Figures 1, 2, and 6. This supports the hypothesis that A80/20m, and by extension the gels formed at higher protein concentration but under the same gelling conditions (G80/20m), follows scheme 2.

The anomalous solubility behavior of G65/60m in Figure 2, with an estimated pK of ∼10.3, parallels the base denaturation of unheated βLg. At low-gelation temperatures, gels are formed mainly by thiol-disulfide bond exchange reactions.[17,32,33] Noncovalent interactions, like intermolecular β-sheets,[20] are not extensive, probably because of the limited extent of denaturation.[17] Therefore, the small clusters that are formed behave like unheated monomers in the presence of alkali. On the other hand, it is not clear that the differences in solubility observed in gels formed at higher temperatures and longer gelling times (G80/5m, G80/20m, and G90/45m, Figure 2), together with the much slower breakdown reactions in the aggregates A80/24h (Figure 7), are related to a higher presence of noncovalent interactions. Only the λ_{max} transition seems to shift at higher pH for A80/24h compared to A80/20m (Figure 9b); there is no statistical difference in the other parameters analyzed. A more plausible explanation, in our opinion, is that the increasing concentration of intermolecular disulfide bonds at higher temperatures and longer gelling times impedes the breakdown of the noncovalent interactions. Shimada and Cheftel[13] argued

that hydrophobic interactions stabilized by disulfide bonds may produce gels with very low solubility in buffers lacking DTT. Eventually, the disulfide bridges would become important enough that their destruction becomes necessary for the breakdown of the protein clusters, which we believe to occur in A80/24h, described as scheme 3.

The present study suggests that the onset of dissolution, and therefore solubilization, of βLg gels formed at gelling times which are not too long (80 °C for 20−60 min are typical conditions) is related exclusively to the breakdown of noncovalent interactions (i.e., scheme 2). Intermolecular disulfide bonds do not seem to be relevant because of their reduced presence. For example, the fact that so few large aggregates remain after 1 h or less of exposure at pH 12 and 20 °C for A80/20m (Figure 5a), when the β-elimination reaction is very slow at this pH and temperature, suggests that the large aggregates were not highly covalently cross-linked. This agrees with the hypothesis that in the growth of large aggregates from small oligomers,[34] noncovalent interactions play a key role, as shown by Bauer et al.[35] Noncovalent interactions become more important at higher protein concentrations[36] and at high temperatures.[17]

However, the solubility data in the presence of denaturants, which are commonly used to estimate the fraction of covalently cross-linked aggregates, suggest a much higher presence of disulfide bridges. As reported previously, G80/20m is only 40% soluble in the presence of denaturants.[14] A large proportion of large aggregates was also observed when A80/20m and A80/24h were incubated overnight in urea or GuHCl (Figure 8), which is a much longer incubation time than the 1−2 h for the solubility experiments with phosphate buffers. βLg unfolding in urea is complete above 6 M,[37,38] and above 4 M in GuHCl,[37] even for oligomers.[26] Therefore, it seems that the ability of urea to destroy hydrogen bonds and to weaken hydrophobic interactions,[39] or the chaotropic properties of GuHCl, is not sufficient to destroy all the noncovalent bonds of the aggregates, whereas alkali at pH 12 is sufficient and much faster. We suggest that a high pH (>11.5) is more effective in destroying these interactions than urea or GuHCl because of the high protein charge that will greatly enhance interprotein repulsion. At pH 12, the net charge of βLg with its 162 residues is about −30, enough to disrupt most of the secondary structure as noted above and, we suggest, the noncovalent interprotein interactions too. In addition, the higher repulsion allows the clusters to swell extensively,[12] and the increased free volume would facilitate the disentanglement, from a traditional polymer physics perspective,[8−10] of covalently linked aggregates. However, we emphasize again that our previous analysis of the destruction of intermolecular disulfide bonds is based on the kinetic data obtained for intramolecular bonds. There remains the possibility that the intermolecular bonds are cleaved in alkali much more quickly than the intramolecular ones, and a pH 12 solution would then be more effective than urea or GuHCl because of the reduction of the disulfide bridges. However, if intermolecular disulfide bonds were so easy and quick to cleave at pH 12, new unresolved questions arise, like the much longer breakdown time observed for A80/24h.

While several studies have determined that intermolecular disulfide bond formation plays a relevant role in the aggregation and gelation processes, particularly during the onset of gelation, the extent of the relative contribution of noncovalent interactions once the gel is well formed is not clear,[40] as both interactions are present simultaneously.[18,41,42] On the other hand, noncovalent cross-linked aggregates have been widely reported in the literature.[13,17,18,36,43−45] The present work suggests that the latter are more relevant than previously considered, in agreement with the recent work of Havea et al.,[46] especially for holding the large aggregates together.[35] The common use of denaturants to elucidate the presence of noncovalent interactions via solubility testing may not be a completely effective technique. Micrometer-size particles are formed after the gels are homogenized. Even though the noncovalent interactions in these particles may have been completely destroyed, the final stage where covalently cross-linked chains are detached from these large clusters may be inhibited by physical entanglements from leaving such large particles. This would lead to an overestimation of the insoluble part and thereby estimating a higher proportion of covalently linked aggregates. Moreover, it is intriguing that the effect of urea and GuHCl in different gels (Figure 2) and aggregates (Figure 8) is similar to that of a pH ∼ 11.6 solution, which coincidentally is the value we have found for the mean dissolution pH threshold.

Conclusions

We have demonstrated the existence of a practical dissolution pH threshold in βLg gels, depending on the gelation conditions. For gels with a high amount of noncovalent interactions (formed at 80 or 90 °C), the dissolution threshold is found to lie between pH 11.5 and 11.85. This sharp solubility transition is caused by the base-induced denaturation of βLg aggregates, as monitored with tryptophan fluorescence and CD, which destroys the intra- and interprotein noncovalent interactions. We suggest that the breakup of the noncovalent interactions is related to the high interprotein repulsion at alkaline pHs, where βLg is highly negatively charged, which could also explain the much higher efficiency of a pH 12 solution in destroying large aggregates compared to concentrated solutions of urea or GuHCl. If gels are not stabilized by noncovalent bonds, as those formed at 65 °C for 60 min are not, the increase in solubility with pH resembles that of the base-induced denaturation of unheated βLg. On the other hand, if the aggregates are formed by heating for a long time (80 °C for 24 h), the extensive formation of intermolecular disulfide bonds hinders the subsequent breakdown process, as these bonds have to be cleaved, through a β-elimination mechanism, for satisfactory dissolution of the aggregates.

Acknowledgment. We wish to thank Dr. Victor Bolanos-García and Dr. Ben Luisi at the Department of Biochemistry, University of Cambridge, for their assistance with CD; Dr. Simon Hanslip for his help with SEC; and Salvatore Mascia for stimulating discussions. The provision of βLg by Davisco (United States) and financial support for RM-C from the Cambridge European Trust is also gratefully acknowledged.

References and Notes

(1) De la Fuente, M. A.; Singh, H.; Hemar, Y. *Trends Food Sci. Technol.* **2002**, *13*, 262−274.
(2) Mackie, A. R.; Gunning, P. A.; Wilde, P. J.; Morris, V. J. *J. Colloid Interface Sci.* **1999**, *210*, 157−166.
(3) Lefevre, T.; Subirade, M. *J. Colloid Interface Sci.* **2003**, *263*, 59−67.
(4) Jennings, W. G. *J. Dairy Sci.* **1959**, *42*, 1763−1771.
(5) Mercadé-Prieto, R.; Chen, X. D. *AIChE J.* **2006**, *52*, 792−803.
(6) Leclerq-Perlat, M. N.; Lalande, M. *Int. Chem. Eng.* **1991**, *31*, 74−93.
(7) Tuladhar, T. R.; Paterson, W. R.; Wilson, D. I. *Trans. Inst. Chem. Eng., Part C, Food Bioprod. Process* **2002**, *80*, 199−214.
(8) Papanu, J. S.; Soane, D. S.; Bell, A. T.; Hess, D. W. *J. Appl. Polym. Sci.* **1989**, *38*, 859−885.

(9) Narasimhan, B.; Peppas, N. A. *J. Polym. Sci., Part B: Polym. Phys.* **1996**, *34*, 947−961.
(10) Devotta, I.; Badiger, M. V.; Rajamohanan, P. R.; Ganapathy, S.; Mashelkar, R. A. *Chem. Eng. Sci.* **1995**, *50*, 2557−2569.
(11) Hunek, B.; Cussler, E. L. *AIChE J.* **2002**, *48*, 661−672.
(12) Mercadé-Prieto, R.; Falconer, R. J.; Paterson, W. R.; Wilson, D. I. *Biomacromolecules*, **2007**, In Press; Doi: 10.1021/bm060553n.
(13) Shimada, K.; Cheftel, J. C. *J. Agric. Food Chem.* **1988**, *36*, 1018−1025.
(14) Mercadé-Prieto, R.; Falconer, R. J.; Paterson, W. R.; Wilson, D. I. *J. Agric. Food Chem.* **2006**, *54*, 5437−5444.
(15) Sreerama, N.; Woody, R. W. *Anal. Biochem.* **2000**, *287*, 252−260.
(16) Keim, S.; Hinrichs, J. *Int. Dairy J.* **2004**, *14*, 355−363.
(17) Galani, D.; Apenten, R. K. O. *Int. J. Food Sci. Technol.* **1999**, *34*, 467−476.
(18) Gezimati, J.; Creamer, L. K.; Singh, H. *J. Agric. Food Chem.* **1997**, *45*, 1130−1136.
(19) Matsuura, J.; Manning, M. C. *J. Agric. Food Chem.* **1994**, *42*, 1650−1656.
(20) Lefèvre, T.; Subirade, M. *Biopolymers* **2000**, *54*, 578−586.
(21) Hoffmann, M. A. M.; Van Mil, P. J. J. M. *J. Agric. Food Chem.* **1997**, *45*, 2942−2948.
(22) Whitaker, J. R.; Feeney, R. E. *Crit. Rev. Food Sci. Nutr.* **1983**, *19*, 173−212.
(23) Waissbluth, M. D.; Gieger, R. A. *Biochemistry* **1974**, *13*, 1285−1288.
(24) Taulier, N.; Chalikian, T. V. *J. Mol. Biol.* **2001**, *314*, 873−889.
(25) Renard, D.; Lefebvre, J.; Griffin, M. C. A.; Griffin, W. G. *Int. J. Biol. Macromol.* **1998**, *22*, 41−49.
(26) Carrotta, R.; Bauer, R.; Waninge, R.; Rischel, C. *Protein Sci.* **2001**, *10*, 1312−1318.
(27) Creamer, L. K. *Biochemistry* **1995**, *34*, 7170−7176.
(28) Strasburg, G. M.; Ludescher, R. D. *Trends. Food Sci. Technol.* **1995**, *6*, 69−75.
(29) Ikeda, S.; Nishinari, K. *Biopolymers* **2005**, *59*, 87−102.
(30) Griffin, W. G.; Griffin, M. C. A. *J. Chem. Soc., Faraday Trans.* **1993**, *89*, 2879−2889.
(31) Qi, X. L.; Holt, C.; McNulty, D.; Clarke, D. T.; Brownlow, S.; Jones, G. R. *Biochem. J.* **1997**, *324*, 341−346.
(32) Roefs, P. F. M.; de Kruif, C. G. *Eur. J. Biochem.* **1994**, *226*, 883−889.
(33) Iametti, S.; Cairoi, S.; De Gregori, B.; Bonomi, F. *J. Agric. Food Chem.* **1995**, *43*, 53−58.
(34) Pouzot, M.; Nicolai, T.; Durand, D.; Benyahia, L. *Macromolecules* **2004**, *37*, 614−620.
(35) Bauer, R.; Carrotta, R.; Rischel, C.; Øgendal, L. *Biophys. J.* **2000**, *79*, 1030−1038.
(36) Havea, P.; Singh, H.; Creamer, L. K.; Campanella, O. H. *J. Dairy Res.* **1998**, *65*, 79−91.
(37) Greene, R. F., Jr.; Pace, C. N. *J. Biol. Chem.* **1974**, *249*, 5388−5393.
(38) Busti, P.; Scarpeci, S.; Gatti, C.; Delorenzi, N. *Food Res. Int.* **2002**, *35*, 871−877.
(39) Kokufuta, E.; Suzuki, H.; Yoshida, R.; Yamada, K.; Hirata, M.; Kaneko, F. *Langmuir* **1998**, *14*, 788−795.
(40) Hoffmann, M. A. M.; Sala, G.; Olieman, C.; de Kruif, C. G. *J. Agric. Food Chem.* **1997**, *45*, 2949−2957.
(41) Dalgleish, D. G.; Seranatne, V.; Francois, S. *J. Agric. Food Chem.* **1997**, *45*, 3459−3464.
(42) Gezimati, J.; Singh, H.; Creamer, L. K. *J. Agric. Food Chem.* **1996**, *44*, 804−810.
(43) Mcswiney, M.; Singh, H.; Campanella, O. H. *Food Hydrocolloids* **1994**, *8*, 441−453.
(44) Anema, S. *J. Agric. Food Chem.* **2000**, *48*, 4168−4175.
(45) Manderson, G. A.; Hardman, M. J.; Creamer, L. K. *J. Agric. Food Chem.* **1998**, *46*, 5052−5061.
(46) Havea, P.; Carr, A. J.; Creamer, L. K. *J. Dairy Res.* **2004**, *71*, 330−339.

BM061100L